BILINGUAL PUBLISHING GROUP

Journal of Environmental & Earth Sciences

https://journals.bilpubgroup.com/index.php/jees

ARTICLE

Comprehensive Utilization of Borehole AFET and Logging Method Detecting Goaf Area in Coal Mines

Zipeng Guo

UCHN Energy Investment Group SHEN DONG COAL Geological Survey Company, Ordos 017000, China

ABSTRACT

China, as the world's largest coal producer and consumer, faces increasingly severe challenges from coal mine goaf areas formed through decades of intensive mining. These underground voids, resulting from exhausted resources or technical limitations, not only cause environmental issues like land subsidence and groundwater contamination but also pose critical safety risks for ongoing mining operations, including water inrushes, gas outbursts, and roof collapses. Conventional geophysical methods such as seismic surveys and electromagnetic detection demonstrate limited effectiveness in complex geological conditions due to susceptibility to electrical heterogeneity, electromagnetic interference, and interpretation ambiguities.This study presents an innovative integrated approach combining the Audio-Frequency Electrical Transillumination (AFET) method with multi-parameter borehole logging to establish a three-dimensional detection system. The AFET technique employs 0.1–10 kHz electromagnetic waves to identify electrical anomalies associated with goafs, enabling extensive horizontal scanning. This is complemented by vertical high-resolution profiling through borehole measurements of resistivity, spontaneous potential, and acoustic velocity. Field applications in Shanxi Province's typical coal mines achieved breakthrough results: Using a grid-drilling pattern (15 m spacing, 300 m depth), the method successfully detected three concealed goafs missed by conventional approaches, with spatial positioning errors under 0.5 m. Notably, it accurately identified two un-collapsed water-filled cavities. This surface-borehole synergistic approach overcomes single-method limitations, enhancing goaf detection accuracy to over 92%. The technique provides reliable technical support for safe mining practices and represents significant progress in precise detection of hidden geological hazards in

*CORRESPONDING AUTHOR:

Zipeng Guo, UCHN Energy Investment Group SHEN DONG COAL Geological Survey Company, Ordos 017000, China;
Email: 1542145556@qq.com

ARTICLE INFO

Received: 30 November 2024 | Revised: 26 December 2024 | Accepted: 30 December 2024 | Published Online: 17 April 2025
DOI: https://doi.org/10.30564/jees.v7i5.7934

CITATION

Guo, Z., 2025. Comprehensive Utilization of Borehole AFET and Logging Method Detecting Goaf Area in Coal Mines. Journal of Environmental & Earth Sciences. 7(5): 1–16. DOI: https://doi.org/10.30564/jees.v7i5.7934

Chinese coal mines, offering valuable insights for global mining geophysics.

Keywords: Underground Coal Mine; Goaf; Audio-Frequency Electrical Transillumination (AFET); Gamma Logging; Borehole Imaging

1. Introduction

The long-term mining of coal in China has led to a large number of coal mine goafs. The unclear and uncertain location of goaf areas is a challenge for the coal mining in China. Once the goaf collapses during the mining process, it not only affects the geological environment but also endangers people's property and even life safety. To ensure the safety of mining, it is necessary to carry out goaf area detection before mining[1–3].

The geophysical exploration methods are used for the detection and analysis of goaf areas. The main methods for detecting goaf areas are as follows:

1. Seismic exploration[4], where seismic waves are generated on the surface or underground and reflected or refracted back to the receivers. The travel time and amplitude of the seismic waves are analyzed to infer subsurface structures. This method provides high-resolution images of subsurface structures, suitable for large-scale exploration. However, this method is high cost, sensitive to environmental noise, and requires specialized knowledge for data interpretation. When the goaf area is composed of goaf tunnels, which are relatively small in size, they cannot be detected using seismic exploration.
2. Electromagnetic exploration[5], where electromagnetic waves are emitted and their propagation characteristics are measured underground. The attenuation and phase changes of the waves are used to infer formation structures. This method is sensitive to water content in goaf areas, real-time monitoring is possible, and the equipment is lightweight. However it is heavily influenced by surface conditions and has limited detection capability for dry goaf areas. The detection accuracy of this method is limited, and the detection depth is also limited, making it impossible to achieve accurate detection.
3. Magnetic exploration[6], which measures changes in the Earth's magnetic field on the surface to infer changes in the magnetic properties of underground rocks. It is sensitive to the distribution of magnetic minerals and can be used to identify the boundaries of goaf areas. It is heavily influenced by surface magnetic interference, with limited detection capability for non-magnetic rock goaf areas.
4. High-density resistivity methods[7, 8], where current is applied on the surface, and potential differences are measured. Changes in resistivity are used to infer subsurface structures.It is sensitive to changes in moisture and geological structure of goaf areas. It is heavily influenced by surface conditions and groundwater flow, and data interpretation is complex. The detection accuracy of this method is limited, and the detection depth is also limited, making it impossible to achieve accurate detection.
5. Ground-penetrating radar[9], where high-frequency electromagnetic waves are emitted and received by antennas. Reflected waves' delay and intensity are analyzed to detect subsurface structures. It provides continuous subsurface profiling with high resolution, suitable for shallow exploration. However, it has limited detection depth, is sensitive to electromagnetic interference, and is less effective for wet goaf areas. When it is used in underground coal mines, it is inconvenient for detecting the goaf in the upper part and in front of the roadway during construction.
6. Borehole logging[10]. Logging instruments are lowered into boreholes to measure the physical properties of rocks, such as density, porosity, resistivity, etc. It provides direct data on the physical properties of underground rocks, suitable for detailed exploration. This method has a short detection radius and cannot be directly used for goaf detection.
7. Gravity exploration[11]. It measures changes in gravity on the surface to infer changes in underground mass distribution. It is not limited by surface conditions, making it suitable for large-scale exploration. However, it has low sensitivity to small-scale or local changes and requires high-precision instruments. This method is not suitable for high-precision detection of goaf areas.

To summarize, there are inaccuracies in the boundaries of goaf areas detected by seismic exploration, transient electromagnetic detection methods, and magnetic prospecting methods; the detection depth of high-density electrical methods and ground-penetrating radar detection methods is limited. The borehole logging and gravity exploration are not suitable for goaf area detection directly. Moreover, as the scale and depth of coal mining continue to increase, goaf detection faces unfavorable factors such as complex geological and filling conditions, and numerous interference factors in the detection area. There is an urgent need to study new detection methods to detect the goaf accurately.

Audio-frequency electrical transillumination(AFET) technology is a geophysical method that combines the principles of electrical resistivity tomography and seismic tomography to image subsurface structures. It works on the basis of the differences in electrical conductivity and electromagnetic wave velocity within the subsurface. It has been widely applied in the detection of water-containing areas within the working faces in coal mine tunnels, while cross-hole AFET has seen extensive use in the detection of karst in engineering surveys[12–19]. It has also achieved good results in the detection of boundaries of goaf areas in coal mines for the management of railway diseases on the ground[20]. However, cross-hole AFET is not used in the detection of goaf areas underground in coal mines, mainly because the underground boreholes in coal mines are nearly horizontal, and the geological conditions around the boreholes are asymmetric. Logging detection has a high degree of precision, yet due to the limited detection radius, it has not been utilized for goaf detection. This paper conducts a study on the propagation law of electromagnetic waves in the perspective detection of goaf using AFET under an asymmetric geological model, then proposes the use of boreholes in coal mines to comprehensively employ AFET and multi-parameter logging technology for the detection of goaf boundaries. Finally, it provides a practical method for comprehensive application to illustrate how this method is used.

2. Characteristics of AFET in Asymmetric Strata

The method of using AFET to detect goaf in boreholes refers to emitting electromagnetic waves in one hole and receiving electromagnetic waves in another hole to detect the goaf between two boreholes, as shown in **Figure 1**. The detection between the two boreholes is achieved by using the difference in absorption and attenuation of electromagnetic waves in different media. The received data is processed by tomography to obtain the electromagnetic wave absorption and attenuation distribution map, which is used to determine the distribution of electrical properties between the two boreholes and indirectly achieve the purpose of exploring the goaf[21].

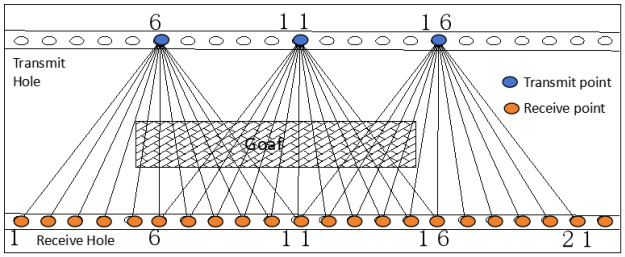

Figure 1. Schematic diagram of borehole AFET of goaf.

For AFET data, the objective function form of the three-dimensional inversion problem is as follows[22, 23]:

$$\varnothing(\mathrm{m}) = \frac{1}{2}||\mathrm{d}(\mathrm{m}) - \mathrm{d}_{\mathrm{obs}}||^2 + \frac{\beta}{2}||\mathrm{W}(\mathrm{m} - \mathrm{m}_{\mathrm{ref}})||^2 \quad (1)$$

Where $\mathrm{d}_{\mathrm{obs}}$ are measured data; $\mathrm{d}(\mathrm{m})$ is the data obtained by forward modeling a given conductivity model; the second term in the above equation is the Tikhonov regularization term, which contains existing prior information; β is a regularization parameter used to balance the impact of data errors and model regularization during the minimization process; W is the model regularization matrix; m is a model used for inversion iteration, with model parameters taken as the natural logarithm of conductivity $\ln(\delta)$; $\mathrm{m}_{\mathrm{ref}}$ is a reference model. The first term of the objective function ensures that the inversion model matches the observed data, while the second term strengthens the prior information about the model shape, structure, etc. based on the model The pseudo Gaussian Newton method is used to invert and fit the objective function, obtaining the best model that matches the observed data. This model approximately reflects the electrical distribution of geological structures underground in coal mines. The specific data processing methods are as follows:

Firstly, define the initial model m_i, which generally uses a uniform model composed of the measured background conductivity of the area as the initial model Linearize Equa-

tion (1) based on this model, we can get the:

$$\varnothing(\mathrm{m}) = \frac{1}{2}||(\mathrm{d} - \frac{\partial \mathrm{d}}{\partial \mathrm{m}} \cdot \delta \mathrm{m})\mathrm{d} - \mathrm{d}_{\mathrm{obs}}||^2 + \frac{\beta}{2}||\mathrm{W}(\mathrm{m} - \mathrm{m}_{\mathrm{ref}})||^2 \quad (2)$$

To obtain the minimum value of $\varnothing(\mathrm{m})$, take the derivative of the model parameters using the above formula and make them zero, to obtain the updated formula for the Gauss Newton method:

$$(J^T J + \beta W^T W) \cdot \delta n = -(J^T(QA^{-1}q - d_{obs}) + \beta W^T W\,(m - m_{ref})) \quad (3)$$

Among them, $J = \partial d/\partial m$ is the Jacobian matrix or sensitivity matrix; $g = (J^T(QA^{-1}q - d_{obs}) + \beta W^T W(m - m_{ref}))$ is the gradient of the objective function; $H = \left(J^T J + \beta W^T W\right)$ is an approximate Hessian matrix. The model update is obtained by solving the following linear system:

$$\delta m = -H^{-1} \cdot g \quad (4)$$

H and J are both large dense matrices, and whether solved using direct or iterative methods, it will result in a huge computational load In order to obtain effective model updates, both $\boldsymbol{J}$ and H^{-1} do not require high-precision solutions, and low precision approximations are made to each linear system during the solution process.After obtaining the model update, a new model can be established:

$$m_{i+1} = m_i + \alpha \delta m \quad (5)$$

In the equation, α is a linear search parameter used to control the magnitude of model updates Here, α is selected based on the *Armijo* criterion:

$$\varnothing(m_{i+1}) = \varnothing(m_i + \alpha \delta m) \geq \varnothing(m_i) + c_1 \alpha \nabla \varnothing^T(m_i) \delta m \quad (6)$$

Among them, c_1 is a constant with a very small value (approximately equal to 10^{-4}). The above formula ensures that model updates can effectively reduce the objective function when calculating the new model of Equation (5), the initial value of α is taken as 1; after obtaining the new model, calculate Equation (6); if the inequality holds, accept the new model; if it does not hold, halve the value of α and recalculate Equation (5); repeat the above process until the new model meets the discrimination criteria of Equation (6).

Since Equation (5) is obtained by linearizing m_i, the new model m_{i+1} may not necessarily be the global optimal solution, and it is necessary to re-linearize m_{i+1} and perform another update iteration; repeat the above iterative process until the objective function or data error is reduced to an acceptable level In addition, when the gradient g of the objective function decreases to a given threshold, the inversion can be stopped, which means that the objective function has already been smoothed and no further improvements can be made to the model.

Due to the asymmetry of the surrounding strata in the coal mine underground near horizontal boreholes, there is a significant difference from the vertical hole on the ground. In order to analyze the distribution characteristics of electromagnetic fields in the detection of goaf in coal mine boreholes using AFET, we established a 3D model with the size of 10 m × 10 m × 9 m. From top to bottom, the first layer is shale with a thickness of 2 m, the middle layer is coal seam with a thickness of 5 m, and the lower layer is sand with a thickness of 2 m. The electrical conductivity of shale, coal, and sand is 0.005 S m^{-1}, 0.001 S m^{-1}, and 0.01 S m^{-1}, respectively. The relative dielectric constants of shale, coal, and sand are 8, 4, and 6, respectively. The porosity of shale, coal, and sand is 0.005, 0.001, and 0.01, respectively.The relative magnetic permeability of shale, coal, and sands are 1. The goaf is filled with water and has a size of 2 m × 2 m × 2 m.

Firstly the transmission borehole is a horizontal hole along the coal seam, at a distance of 1 m from the coal seam bottom interface. We set 9 signal transmission points in the transmission borehole, as shown in **Figure 2**.

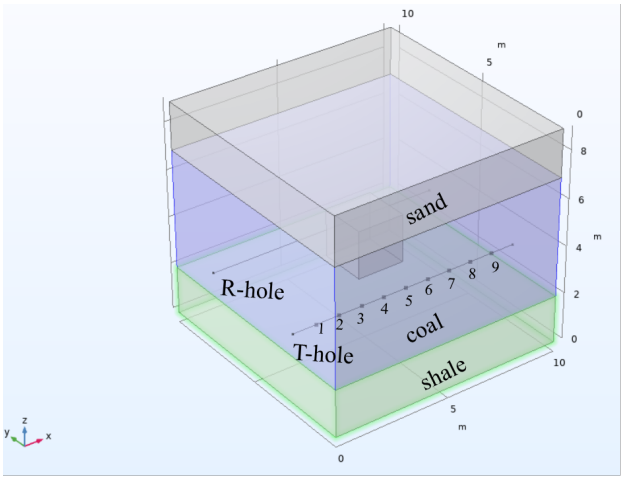

Figure 2. The 3D model for horizontal hole.

Note: T-hole is an electromagnetic wave signal transmission borehole. R-hole is an electromagnetic wave signal receiving borehole. Numbers 1–9 are 9 points of electromagnetic wave emission, with an interval of 1 m between each point.

The distribution of electromagnetic induction lines in the formation (Slice on the xz plane at the center position of the model) is shown in **Figure 3** when emitting electromagnetic signals at 9 different emission points.

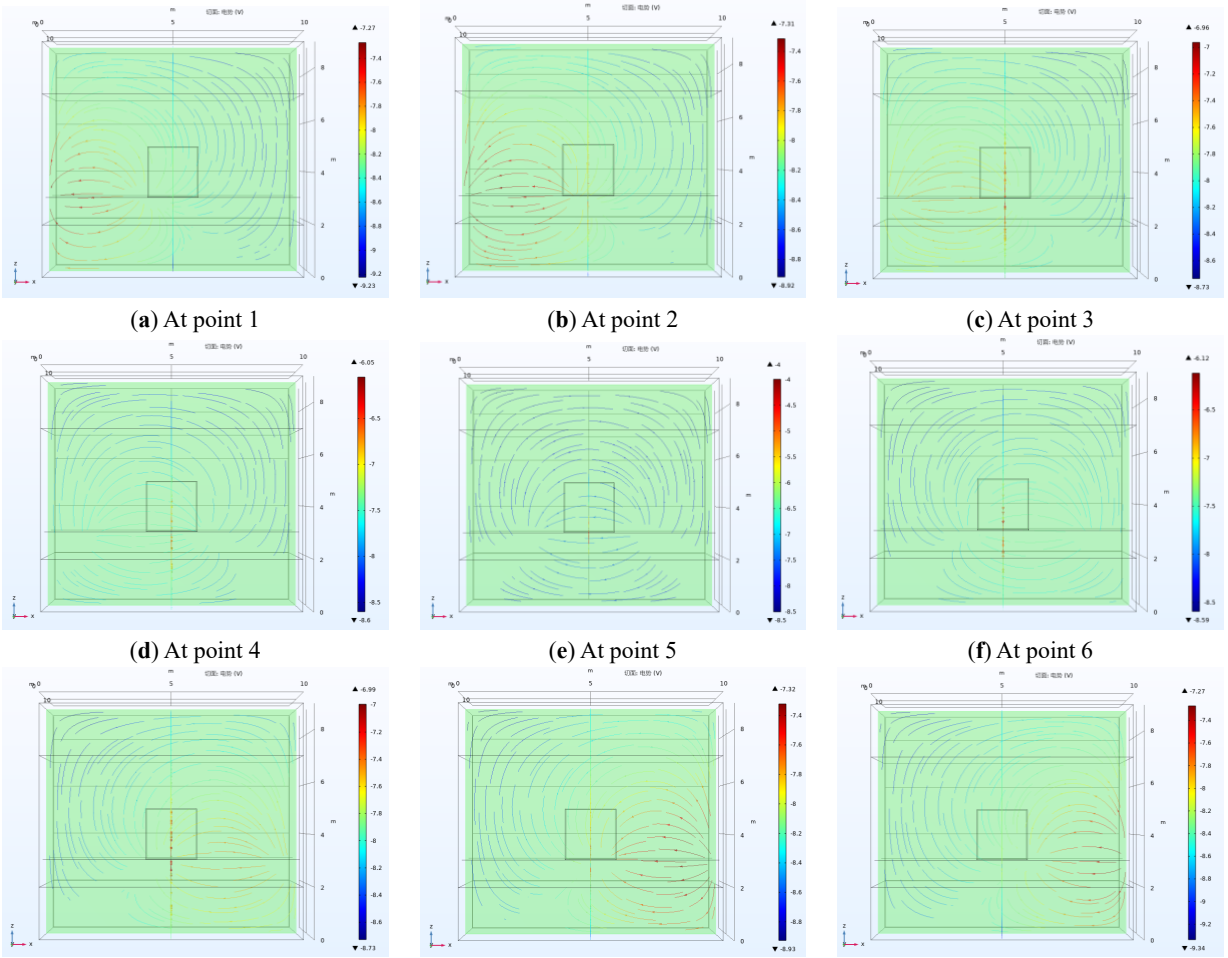

(**a**) At point 1 (**b**) At point 2 (**c**) At point 3

(**d**) At point 4 (**e**) At point 5 (**f**) At point 6

(**g**) At point 7 (**h**) At point 8 (**i**) At point 9

Figure 3. The distribution of electromagnetic lines at 9 different emission positions in horizontal hole.

Figure 3, which consists of (**a**) through (**i**) a total of 9 sub-figures, illustrates the variation characteristics of electromagnetic waves as they pass through a goaf area within a coal seam when emitted from different points. Based on the comparison of **Figure 3a–i**, which total nine images, aside from the signal emitted from the center point of the borehole, the two electromagnetic signal distribution diagrams that are symmetrically positioned on either side of the center point exhibit symmetrical characteristics. Therefore, it can be simplified to compare only **Figure 3a–e**. In the figures, the distribution characteristics of the equipotential lines are indicated, with arrows on the lines representing the direction of the electric potential, and colors indicating the magnitude of the potential, where red signifies a higher potential and blue signifies a lower potential. By comparing **Figure 3a** with **Figure 3e**, it is observed that when the electromagnetic signal emission point is closer to the goaf area, the distribution of the entire electromagnetic field's potential is weakened, tending towards blue.

It can be seen that when the goaf is located in the coal seam, the electromagnetic waves passing through the goaf will vary for different electromagnetic wave signal emission points. Therefore, the detection of the goaf can be carried out through electromagnetic wave cross hole detection.

Secondly we designed an inclined borehole with the starting point aligned with the horizontal hole above, and the endpoint located in the sandstone layer. We set 9 signal transmission points in the transmission borehole, as shown

in **Figure 4**.

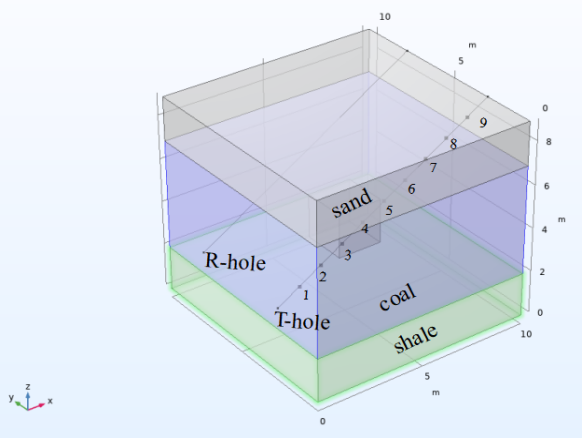

Figure 4. The 3D model for inclined hole.

Note: T-hole is is an electromagnetic wave signal transmission borehole. R-hole is an electromagnetic wave signal receiving borehole. Numbers 1–9 are 9 points of electromagnetic wave emission, with an interval of 1 m in the x-axis direction between each point.

In **Figure 5a–i**, the distribution characteristics of the equipotential lines are indicated, with arrows on the lines representing the direction of the electric potential, and colors indicating the magnitude of the potential, where red signifies a higher potential and blue signifies a lower potential as in **Figure 3a–i**. Comparing the electromagnetic wave distributions in **Figures 5** and **3**, it can be seen that for asymmetric formations around the borehole, when the signal transmission point is located in the coal seam but adjacent to the interface between the coal seam and sandstone at positions 5 and 6 in **Figure 4**, or has already passed through the coal seam and entered the sandstone layer at positions 7, 8, and 9 in **Figure 4**, the propagation of electromagnetic waves undergoes significant changes, and the electromagnetic signals that can pass through the goaf are very weak. In this case, using AFET in the borehole is not a good choice.

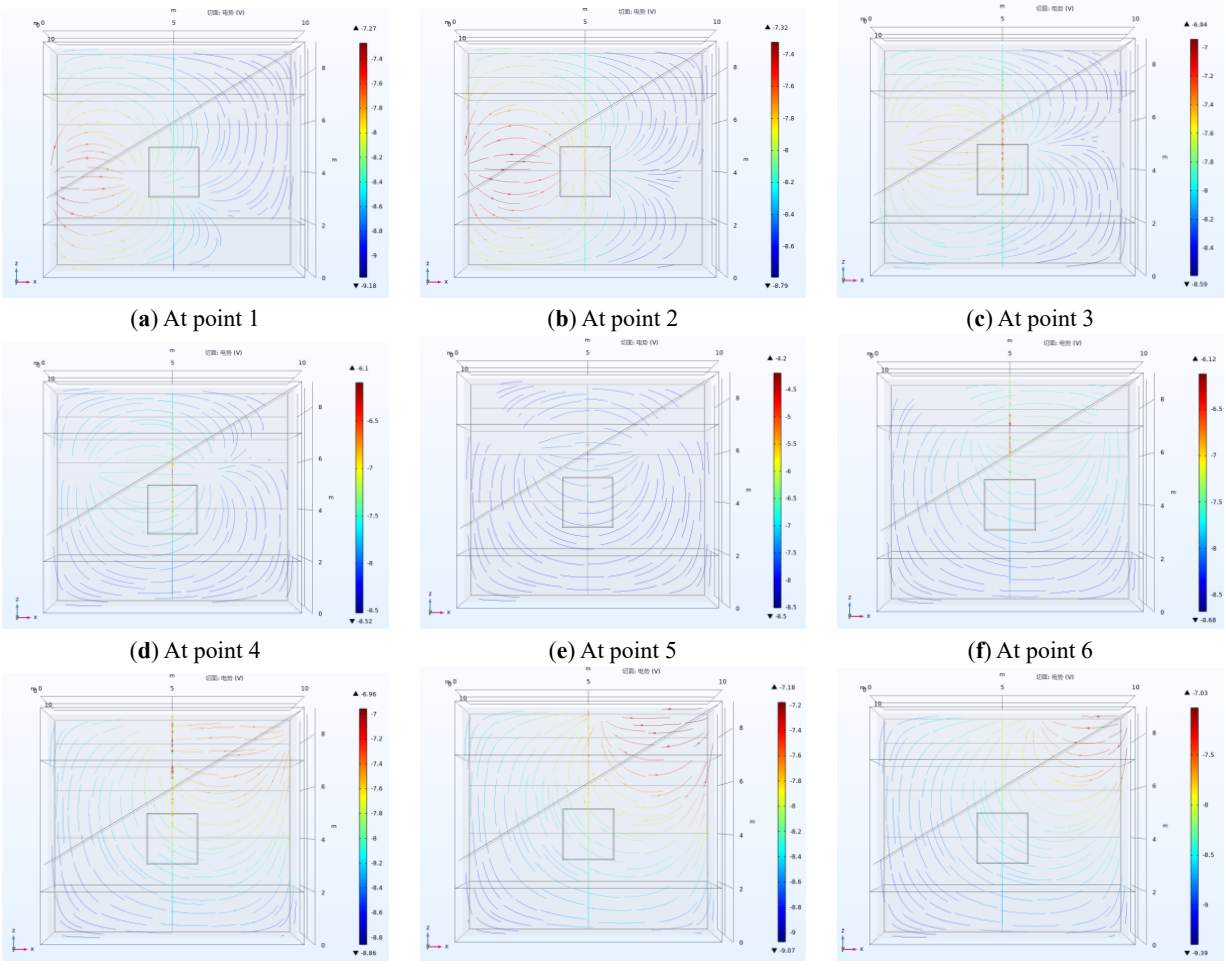

(**a**) At point 1 (**b**) At point 2 (**c**) At point 3

(**d**) At point 4 (**e**) At point 5 (**f**) At point 6

(**g**) At point 7 (**h**) At point 8 (**i**) At point 9

Figure 5. The distribution of electromagnetic lines at 9 different emission positions in inclined hole.

Therefore, when using AFET to detect goaf in coal seams during underground borehole in coal mines, it is advisable to choose boreholes located in the coal seam as much as possible.

3. The Multi-Parameter Logging Method

In order to ensure the selection of suitable boreholes for goaf detection, it is necessary to investigate the borehole conditions. Parameter logging is a multi-parameter logging tool that integrates borehole trajectory measurement, natural gamma logging, and borehole imaging technology. It can measure the trajectory of the borehole, lithology changes along the borehole, and images around the borehole wall.

Borehole imaging technology involves installing a camera and a wide-angle lens with an automatically adjustable aperture into a waterproof pressure chamber, and then placing it into the hole to be detected. The example hole image are shown in the **Figure 6**. The panoramic images of the surrounding and lower parts of the hole wall captured are transmitted through cables to the hole monitor for display. The detection personnel can then view the images of the surrounding hole wall in real time, and the entire detection process is recorded by a video recorder. The camera can also record some images as needed, and the signals around the hole wall are captured by the camera and transmitted to the host through cables and electronic transmission equipment. This technology is mainly used for the division of geological structures, discrimination of wellbore fractures and karst development [24].

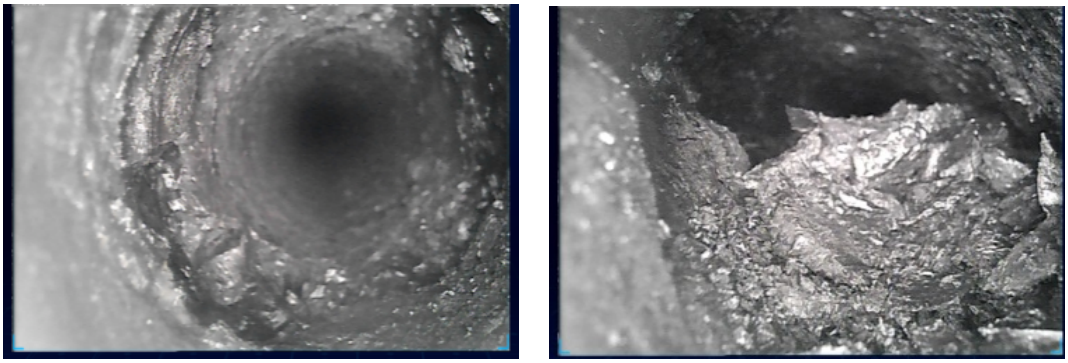

Figure 6. Hole image.

The principle of natural gamma logging in coal mines is that gamma rays in the formation reach the detector, which amplifies them into electrical pulses to form electrical signals, and then converts them into the number of electrical pulses per minute (intensity) for recording. Due to the different lithologies of the strata and the varying levels of radioactive substances contained, the intensity of the gamma rays emitted will differ. Therefore, based on the intensity changes of natural gamma rays in the strata, it is speculated that there will be changes in the lithologies and structures of the strata [25].

The principle of borehole trajectory measurement is to use inertial devices such as gyroscopes and accelerometers to measure the inclination and azimuth of the borehole trajectory, and to achieve synchronous recording of the measurement depth through a hole synchronizer, calculating the spatial position of the measured borehole [24].

The method of analyzing the lithology of geological strata through gamma curve judgment is as follows [26, 27]:

Firstly, it is necessary to smooth the gamma curve to eliminate interference noise. The five-point cubic smoothing method can be used the five-point three-order smoothing method can achieve smoothing of data on equidistant nodes to eliminate the influence of noise signals and improve the quality of logging data. The measurement acquisition sequence *Yi* is The formula for five point three smoothing is:

$$\begin{aligned}
\overline{Y_{i-2}} &= \tfrac{1}{70}(69Y_{i-2} + 4Y_{i-1} - 6Y_i + 4Y_{i+1} - Y_{i+2}) \\
\overline{Y_{i-1}} &= \tfrac{1}{30}(2Y_{i-2} + 27Y_{i-1} + 12Y_i - 8Y_{i+1} + Y_{i+2}) \\
\overline{Y_i} &= \tfrac{1}{35}(-3Y_{i-2} + 12Y_{i-1} + 17Y_i + 12Y_{i+1} - 3Y_{i+2}) \\
\overline{Y_{i+1}} &= \tfrac{1}{35}(2Y_{i-2} - 8Y_{i-1} + 12Y_i + 27Y_{i+1} + 2Y_{i+2}) \\
\overline{Y_{i+2}} &= \tfrac{1}{70}(-Y_{i-2} + 4Y_{i-1} - 6Y_i + 4Y_{i+1} + 69Y_{i+2})
\end{aligned} \tag{7}$$

Where $\overline{Y_i}$ is the improvement value of Y_i.

Secondly, the natural gamma curve is analyzed, and the variance extremum method is used for automatic strat-

ification. The stratification position, i.e., the interface, is determined by calculating the maximum and minimum values of the gamma curve variance.

The essence of stratified analysis of variance is to identify the point with the highest inter layer variance and the lowest intra-layer variance as the stratification point. For two layers of media, assuming there are a total of N sampling points, and X_{1j}, X_{2j} are the logging values of the second point in these two layers, if the layer interface is between the sampling points *n* and *n+1*, then S the sum of the intra-layer differences between the two layers is

$$\begin{gathered} S = \sum_{j=1}^{n}(X_{1j}X_1)^2 + \\ \sum_{j=n+1}^{N}(X_{2j}X_2)^2 = \sum_{j=1}^{n} X_{1j}^2 + \\ \sum_{j=n+1}^{N} X_{2j}^2 nX_1^2\,(Nn)\,X_2^2 = \sum_{j=1}^{N} X_j^2 Q\,(n) \end{gathered} \tag{8}$$

Where:

$$\begin{gathered} X_1 = \frac{1}{n} \times \sum_{j=1}^{n} X_{1j} \\ X_2 = \frac{1}{Nn} \times \sum_{j=n+1}^{N} X_{2j} \\ Q\,(n) = \frac{1}{n} \times \left(\sum_{j=1}^{n} X_{1j}\right)^2 + \frac{1}{Nn} \times \left(\sum_{j=n+1}^{N} X_{2j}\right)^2 \end{gathered} \tag{9}$$

When *N* is constant, the first term in the above equation is a constant, *Q*(*n*) is a function of (*n*, *n+1*) the sequence numbers of the two layered data on both sides of the layer interface, and *Q*(*n*) can reflect the variation law of *S,* the sum of squared differences between the two layers, that is, the larger is *Q*(*n*), the smaller is S; the smaller is *Q*(*n*), the larger is S. At the same time, there is a certain variation pattern on both sides of the layer interface: when $X_1 > X_2$, $X_n > X_{n+1}$; or $X_1 < X_2$, $X_n < X_{n+1}$, there is a maximum value of *Q*(*n*) at the layer interface; when $X_1 > X_2$, $X_n < X_{n+1}$, or $X_1 < X_2$, $X_n > X_{n+1}$ there is a minimum value of *Q*(*n*) at the layer interface. Therefore, by determining the location of the maximum and minimum values of *Q*(*n*) obtained, the hierarchical position can be determined.

Thirdly: After stratification using the variance extremum method, solve for the logging values of each interval. For gamma logging curve, use the average of all data points in that interval as the logging value for that formation. Due to the different distribution of gamma values for different rock types, the corresponding rock type can be determined based on the magnitude of gamma values for each layer. The results obtained by analyzing the lithology along the borehole through gamma value distribution are shown in **Figure 7**.

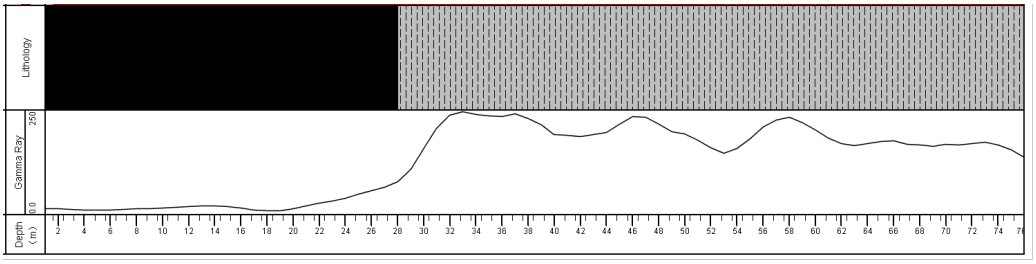

Figure 7. Lithology along the borehole from Gamma logging curve.

4. Comprehensive Detection Method

The method of comprehensively utilizing AFET and multi-parameter logging to detect goaf in borehole is based on the previous geological exploration.The comprehensive detection method work flow is shown in **Figure 8**.

1. Based on the data from previous geological exploration and coal mining in the region, holes are designed according to the detection requirements of the goaf, and then drilling is carried out according to the designed hole trajectory.
2. Using multi-parameter logging to detect each borehole, analyzing the actual borehole trajectory, changes in formation lithology along the borehole, etc.
3. Based on the actual drilling trajectory and rock type changes detected by each borehole, select the boreholes suitable for AFET detection. It is required that each group of electromagnetic wave signal emitting boreholes and electromagnetic wave signal receiving boreholes are on the same plane, and the rock type of the boreholes should be consistent.
4. Use the AFET detection method to detect the selected groups of boreholes, process and analyze the data detected by AFET, and analyze whether there are goaf areas between the detected boreholes.
5. Drill and verify the areas with goaf detected by AFET,

and use the camera of a multi parameter logging tool for observation and verification to ensure the accuracy of the detection.

6. Report the distribution of goaf detection results to the mining party, and the mining owner will determine the next steps of the work plan based on the detection results.

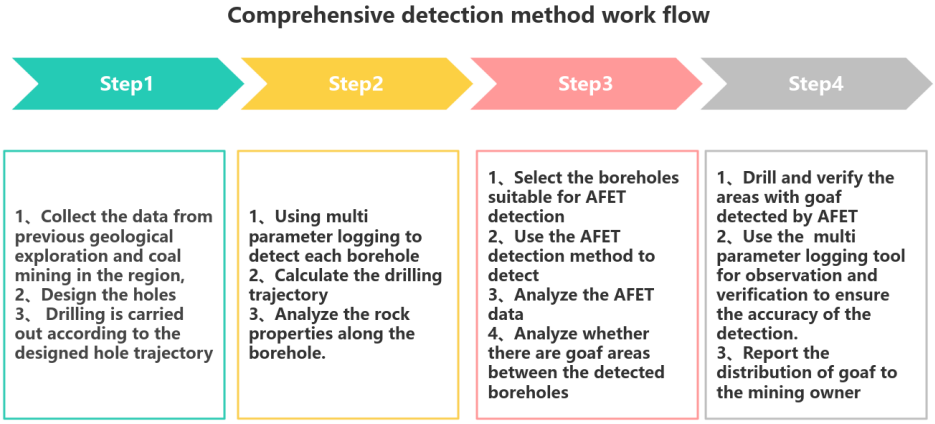

Figure 8. The comprehensive detection method work flow.

5. Application

The actual exploration area in a mining area in Shaanxi Province is 292 m in the east-west direction and 130 m in the north-south direction, with an average coal thickness of 9.0 m. Due to the long mining time and problems with coal mining methods and processes, the thickness and occurrence status of the remaining coal seams in the goaf area are unclear, and there is no detailed geological and hydrogeological data. This has an impact on the mining of the working face, and in the actual process of determining the boundary of the goaf, there is difficulty in determining the boundary of the goaf area. Therefore, before mining the working face, boreholes are drilled in the roadway, and multi-parameter logging instruments and AFET are used for detection of goaf area.

AFET is an instrument that emits electromagnetic waves with a frequency of 30 MHz and receives 30 MHz borehole audio electroporation at the receiver,the instrument is shown in **Figure 9**. The instrument parameters are as listed in **Table 1**. The YZD12 multi parameter logging tool is used for multi parameter logging, which can measure the borehole trajectory, video images along the borehole, and natural gamma,shown in the **Figure 10**. The instrument parameters are as listed in **Table 2**.

Figure 9. The AFET instrument.

Table 1. The parameters of AFET instrument.

Number	Parameters Name	Values
1	Length	1.4 m
3	Diameter	42 mm
4	Transmission frequency	30 MHz
5	Weight	2 Kg
5	Working time	8 h
6	Applicable aperture	>75 mm
7	Applicable hole depth	<200 m
8	Applicable hole spacing	<20 m

Table 2. The parameters of YZD12 multi parameter logging tool.

Number	Parameters Name	Range	Absolute Error
1	Gamma ray counting rate	0–2500 CPS	≤5%
2	Dip	–90°–90°	±0.3°
3	Azimuth	0°–360°	±1.5°
4	Applicable hole depth	<200 m	≤1 m
5	Image	Color: Colorful; Resolution: ≥700 Lines; LED light source illumination: ≥1000 Lux	
6	Length	68 cm	
7	Diameter	42 mm	
8	Weight	4 Kg	

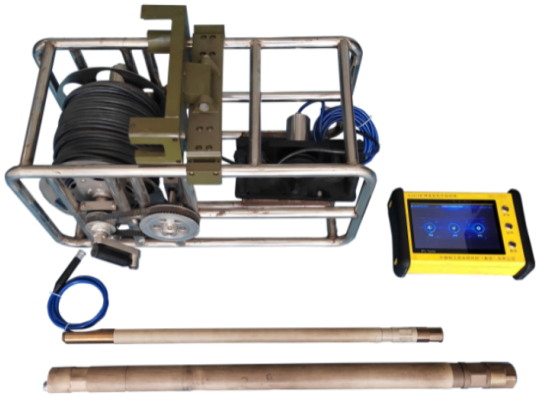

Figure 10. YZD12 multi parameter logging tool.

Based on the results of previous explorations using other methods, there may be a goaf area within a 150 m*50 m region of this coal mine. Ten boreholes were designed in the roadway to explore the boundaries of the goaf. All ten boreholes were designed to face east and were designed as horizontal boreholes. The plane distribution of boreholes is shown in **Figure 11**. Taking the position of borehole 1 as the reference point, the distances between boreholes 2 # to 10 # and borehole 1 # on the plane are 31 m, 44 m, 53 m, 66 m, 85 m, 110 m, 120 m, 137 m, and 152 m, respectively. Firstly, use a multi parameter logging tool to measure the trajectory and lithology of each borehole, and then select the borehole for **AFET** detection. The gamma logging results of 10 boreholes are shown in **Table 3** below. The image of gamma logging detection lithology distribution is shown in **Figure 12**, and typical borehole images are shown in **Figures 13–16**.

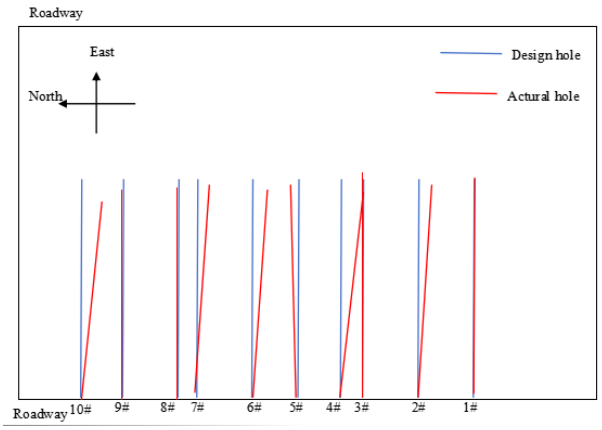

Figure 11. The holes planar distribution.

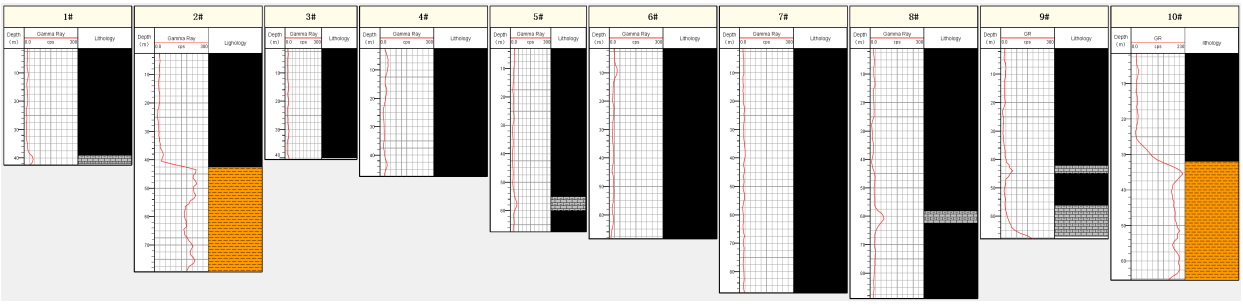

Figure 12. Gamma logging results of the 10 boreholes.

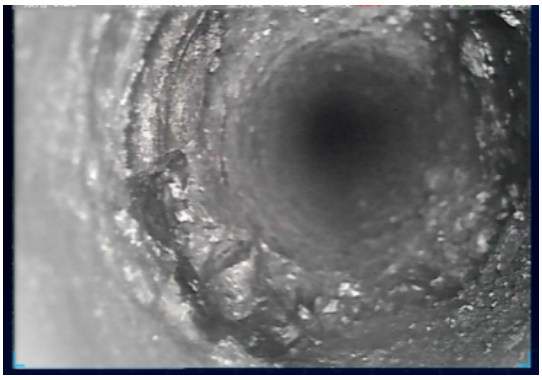

Figure 13. Image of 2 # hole blocked by coal slurry.

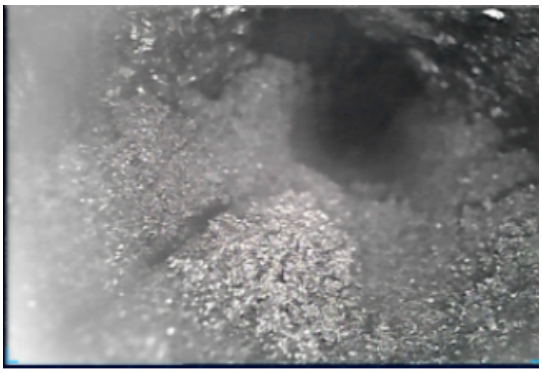

Figure 15. Coal slag image at 58.5 m in hole 5 #.

Figure 14. Image of collapsed hole at 39.5 m in 3 # hole.

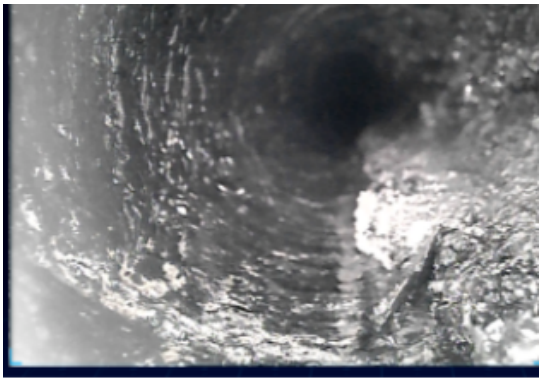

Figure 16. Coal slag image at 25.5 m in hole 10 #.

Table 3. Statistics of measurement data from multi parameter logging tool.

Number	Depth of Hole (m)	Horizontal Offset Distance	Vertical Offset Distance	The Lithology along the Borehole	Video Image Situation
1#	42	Southward 1 m	Up 7 m	0–40 m coal 40–42 m carbonaceous mudstone	The borehole is smooth
2#	78	Southward 13 m	Up 5 m	0–42.5 m coal 42.5 m–78 m shale	There is a lot of coal slurry, and the video image is not clear
3#	52	Southward 8 m	Up 1.25 m	0–52 m coal	There is a lot of coal powder in the hole, and there is a phenomenon of hole collapse
4#	46	Southward 8 m	Up 1.25 m	0–46 m coal	Collapse hole at 44.5 m
5#	70	Northward 4 m	Down 3 m	0–55 m coal 55 m–60 m carbonaceous mudstone 60 m–70 m coal	There is a lot of coal slag in the hole
6#	68	Southward 12 m	Up 2 m	0–68 m coal	There is a lot of coal slag in the hole
7#	70	Southward 16 m	Down 2 m	0–70 m coal	The borehole is smooth
8#	90	Southward 12 m	Up 0.6 m	0–58 m coal 58 m–62 m carbonaceous mudstone 62 m∼90 m coal	There is partial fragmentation
9#	70	Southward 1 m	Down 1 m	0∼42 m coal 42 m∼45 m carbonaceous mudstone 45 m–54 m coal 54 m–68 m carbonaceous mudstone	There is a phenomenon of hole collapse
10#	70	Southward 10 m	Down 2 m	0–32 m coal 32 m–70 m shale	There is a small amount of coal slag inside the hole

Based on the results of multi parameter measurements of boreholes in **Table 3**, select the **AFET** borehole in the coal seam section to ensure that the electromagnetic wave transmission section is not affected by changes in the formation lithology. The boreholes for transmitting and receiving radio wave signals do not intersect on the plane. According to **Figure 11** and **Table 3**, we can get the following knowledge:

1. Borehole No. 1# and Borehole No. 2# are both situated above the drilling start plane, with a vertical distance difference of 2 meters between their final positions. Borehole No. 2# is 13 meters away from Borehole No. 3# at the drilling start point. Both boreholes have a coal section from 0 to 40 meters in depth. At the 40-meter depth, the two boreholes are 7 meters apart. Therefore, these two boreholes can be selected as a pair for AFET detection. One can be chosen as the signal transmitting borehole, and the other as the signal receiving borehole. The detection will focus on the coal layer section between 0 to 40 meters in depth for both boreholes.
2. Borehole No. 4# and Borehole No. 3# intersect horizontally and cannot be selected for AFET detection within these two boreholes. Borehole No. 4# and Borehole No. 2# are both located above the borehole starting plane, with a vertical distance difference of 3.75 meters at the final hole, and the drilling depth from 0–42.5 meters is all coal. The two boreholes are approximately parallel in the plane and are 22 meters apart. Therefore, Borehole No. 4# and No. 2# can be selected as a pair for AFET detection. Choose either one as the signal transmission borehole and the other as the signal receiving borehole. Select the coal seam section from 0–42.5 meters depth in the two boreholes for detection between the two holes to detect the goaf area.
3. Borehole No. 5# is 3 meters downward in the profile, while Boreholes No. 3# and No. 4# are both 1.25 meters upward. On the plane, Borehole No. 5# is approximately parallel to both No. 3# and No. 4#. The depth of 55 meters within Borehole No. 5# is entirely within the coal seam. Therefore, based on the on-site drilling conditions, Borehole No. 5# can be chosen to pair with either No. 3# or No. 4# for AFET detection. Since AFET detection between Borehole No. 2# and No. 4# has revealed characteristics of a goaf area, to further confirm the distribution range of the goaf area between No. 2# and No. 4#, it is decided to conduct AFET detection for the goaf area between Borehole No. 5# and No. 3#.
4. Borehole No. 6#'s final position is 2 meters upward in the cross-section, and it does not intersect with Borehole No. 5# on the plane. The starting positions are 19 meters apart, and the final positions are 3 meters apart. The entire section of Borehole No. 6# is within the coal seam. Since Borehole No. 3# and No. 5# previously detected a goaf area, theoretically, Borehole No. 6# should be chosen with No. 4# for AFET detection. However, due to a collapse at Borehole No. 4#, which prevents detection, Borehole No. 6# is selected to pair with No. 5# for AFET detection to investigate the distribution of the goaf area between these two boreholes.
5. Borehole No. 7#'s final position is 2 meters downward in the cross-section, and it does not intersect with Borehole No. 6# on the plane. The starting positions are 25 meters apart, and the final positions are 21 meters apart. The entire section of Borehole No. 7# is within the coal seam. To ensure the accuracy of AFET detection, the distance between the two boreholes chosen for AFET detection should not be too large. Therefore, Borehole No. 7# is selected to pair with No. 6# for AFET detection to investigate the distribution of the goaf area between these two boreholes.
6. Borehole No. 8#'s final position is 0.6 meters upward in the cross-section, and it does not intersect with Borehole No. 7# on the plane. The starting positions are 10 meters apart, and the final positions are 6 meters apart. The entire section of Borehole No. 8# is within the coal seam. Boreholes No. 7# and No. 8# are too close to each other for AFET detection purposes. Borehole No. 9#'s final position is 1 meter downward in the cross-section, and it is approximately parallel to Borehole No. 8# on the plane. Borehole No. 9#'s starting position is 27 meters away from Borehole No. 8#, and the final positions are 37 meters apart. Additionally, no goaf area characteristics were detected between Boreholes No. 6# and No. 7#. To save detection time and ensure the accuracy of AFET detection, the distance between the two boreholes selected for AFET detection should not be too large. Therefore,

Borehole No. 8# is selected to pair with No. 9# for AFET detection to investigate the distribution of the goaf area between these two boreholes.

7. Borehole No. 10#'s final position is 2 meters downward in the cross-section, and it does not intersect with Borehole No. 9# on the plane. The starting positions are 15 meters apart, and the final positions are 9 meters apart. The depth of Borehole No. 10# from 0–32 meters is within the coal seam. However, the coal seam depth is too small for effective detection, and since no goaf area characteristics were detected during the exploration between Boreholes No. 8# and No. 9#, in order to save detection time, it is decided not to conduct detection near Borehole No. 10#.

Select 6 sets of inter hole AFET detection, including 1 # hole for transmitting and 2 # hole for receiving, 2 # hole for transmitting and 4 # hole for receiving, 3 # hole for transmitting and 5 # hole for receiving, 6 # hole for transmitting and 5 # hole for receiving, 6 # hole for transmitting and 7 # hole for receiving, and 9 # hole for transmitting and 8 # hole for receiving. The absorption attenuation results of borehole audio transmission are shown in **Figures 17–22**.

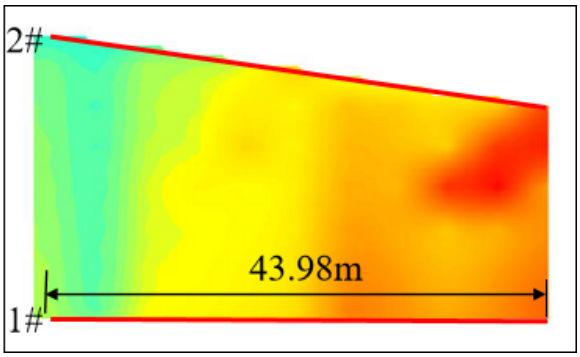

Figure 17. AFET Results between hole 1 # and 2 #.

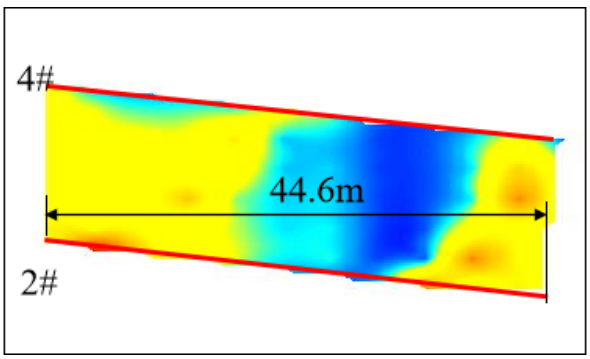

Figure 18. AFET Results between hole 2 # and 4 #.

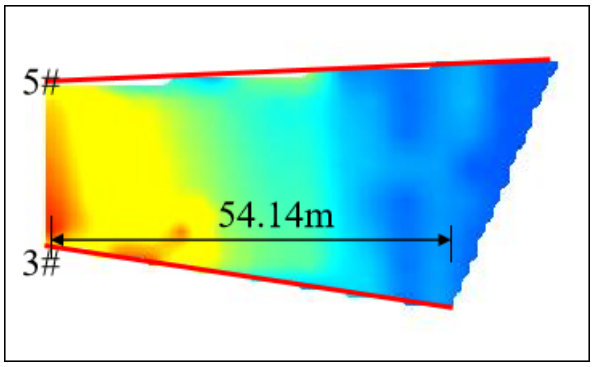

Figure 19. AFET Results between hole 3 # and 5 #.

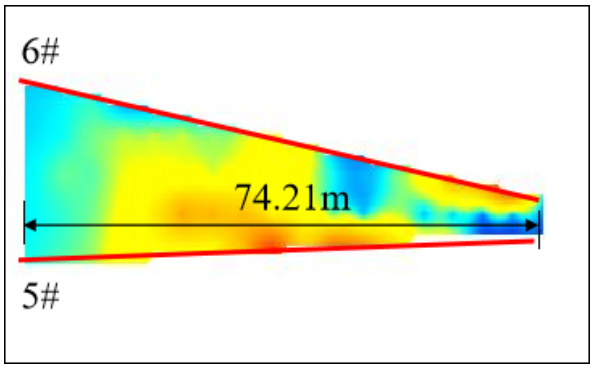

Figure 20. AFET Results between hole 5 # and 6 #.

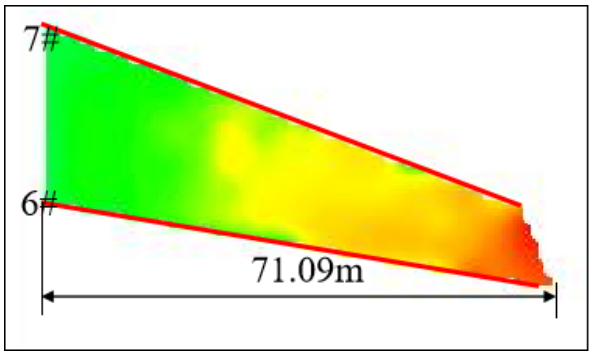

Figure 21. AFET Results between hole 6 # and 7 #.

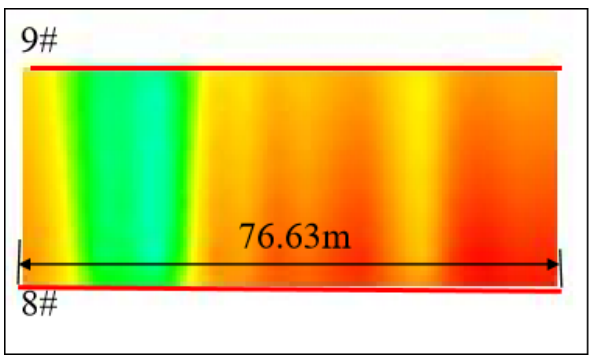

Figure 22. AFET Results between hole 8 # and 9 #.

In **AFET** detection results in borehole in **Figures 17–22**, the red and yellow colors represent high-value areas of electromagnetic wave absorption attenuation (coal seams, mud, sandstone), and the blue-green color represents low value areas of electromagnetic wave absorption attenuation. By comparing with the amplitude of other borehole data in this exploration, the analysis results show that the possibility of goaf in the inter-borehole area controlled by boreholes 1 # and 2 # is relatively small; the blue area between holes 2 # and 4 # is the inferred goaf, and the transition area from blue to green is the inferred edge collapse (semi collapse area) of the goaf; after boreholes 3 and 5 at a depth of 36 m, the goaf developed; the trajectories of boreholes 5 # and 6 # gradually approach from the opening, and when the depth of borehole 6 # reaches 45 m, the signal changes sharply, indicating a reaction from the goaf; there is a low possibility of goaf in the deep part between holes 6 and 7; there are weak goaf anomalies at depths of 12 m to 24 m in boreholes 8 and 9, while no anomalies are observed in other depth areas. Therefore, there exists a goaf area between Borehole No. 4# and Borehole No. 5#, with the goaf area measuring approximately 40 meters in length and 4 meters in width. It is likely to be a tunnel left over from previous mining operations, and this tunnel contains water. Before coal extraction, to ensure safety, it is necessary to deal with the water within this goaf area to prevent safety accidents.

To verify the existence of goaf between boreholes 2 # and 5 # for borehole **AFET** detection, between Borehole No. 2# and Borehole No. 5#, a new borehole is drilled. A multi-parameter logging instrument is then inserted into the borehole. Through the camera on the instrument, a goaf area is discovered (shown as in the **Figure 23**).The morphology of this goaf area is similar to that of a tunnel, which confirms the presence of a goaf area between Borehole No. 2# and Borehole No. 5#, as described earlier, likely caused by a tunnel left from previous mining activities.

Based on the aforementioned analysis, through the design of 10 boreholes, actual drilling, and the use of a multi-parameter logging instrument for trajectory and lithological distribution detection in the boreholes, an AFET detection pair of boreholes was selected. Utilizing AFET detection, one goaf area was discovered, which was then verified through drilling. The potential area of the goaf, which was initially estimated to be 150 m × 50 m, was narrowed down to a range of 40 m × 4 m. Therefore, the combined use of AFET and logging can accurately detect the distribution and location of goaf areas. For a goaf area that is only 4 meters wide, such a small dimension is beyond the capabilities of conventional detection methods to locate with such high precision as described in the introduction.

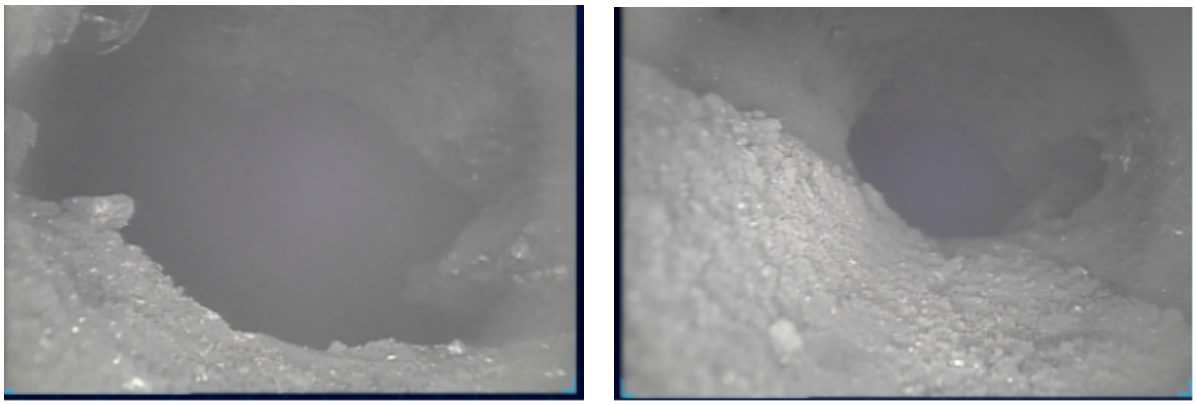

Figure 23. Image of goaf observed in verification borehole.

6. Conclusions

- By establishing a model for detecting goaf using AFET in near-horizontal holes in coal mines, it can be concluded that when AFET is used for goaf detection in parallel horizontal holes, it is not conducive to the detection of goaf when the borehole penetrates the formation where the goaf is located.
- The comprehensive use of multi-parameter logging and AFET can detect goaf area. Firstly, the borehole trajectory measured by multi-parameter logging is used to determine the spatial position of the borehole. Gamma logging is

used to determine the lithological changes along the borehole. Based on the video imaging of the multi-parameter logging instrument, the borehole conditions are observed, and boreholes with spatial positions on the same plane, no intersections on the plane, and consistent lithological ranges are selected for AFET.

- According to actual detection verification, the data from inter-hole audio AFET detection can clearly reflect the distribution of goaf area.

Funding

This work received no external funding.

Institutional Review Board Statement

Not applicable. This study focused on geophysical detection methodologies for coal mine goaf areas and did not involve human participants, animal subjects, or personal data collection. All technical procedures were conducted in compliance with standard engineering practices and geological survey protocols.

Informed Consent Statement

Informed consent is not applicable to this study. This research focused exclusively on geophysical detection methodologies and technical analyses of coal mine goaf areas, with no involvement of human participants, animal subjects, or identifiable personal data.

Written informed consent for publication is not applicable, as the study did not involve clinical cases, patient data, or identifiable individuals

Data Availability Statement

The data that support the findings of this study are derived from actual mine data, which cannot be made publicly available due to privacy and confidentiality restrictions. The data contain sensitive information about the mining operations and related parties that could potentially compromise the security and competitive position of the mining company involved. Access to such data is subject to strict regulations and agreements that prevent us from sharing the raw data outside of the research context.

Acknowledgments

I would like to express my sincere gratitude to *UCHN Energy Investment Group SHEN DONG COAL Geological Survey Company* for their unwavering support throughout the duration of this research project. Their contributions have been instrumental in providing the necessary resources and environment that facilitated the successful completion of my work.

Conflicts of Interest

The authors declare no conflicts of interest.

References

[1] Yang, Y., 2023. Three dimensional forward and backward modeling research and application of frequency domain controllable source electromagnetic method in coal mine goaf [Ph.D. thesis]. Guilin, China: Guilin University of Technology. pp. 20–28.

[2] Liu, W., 2023. Application research of comprehensive geophysical exploration technology in coal mine goaf detection. Energy and Energy Conservation. 05, 193–195+211.

[3] Xiao, L., 2019. Application of comprehensive geophysical methods in goaf detection. Journal of Engineering Geophysics. 16(05), 658–664.

[4] Liu, Y., 2008. Seismic exploration methods on goaf. Coal Technology. 27(4), 100–101.

[5] Fan, T., Li, H., Guo, J., et al., 2020. Application of borehole transient electromagnetic pseudo seismic inversion method in fine exploration of goaf in open-pit coal mines. Journal of Earth Science and Environment. 42(6), 759–766.

[6] Lin, J., Xue, G., Li, B., 2021. Innovative thinking on semi aerial electromagnetic detection method technology. Chinese Journal of Geophysics. 9, 2995–3004.

[7] Liu, K., Wang, Q., Pang, X., 1992. Preliminary experiment of high-density resistivity method. Exploration Science and Technology. 2, 54–56.

[8] Cheng, J., Hu, K., Wang, Y., et al., 2004. Research on ground penetrating radar detection of underground mining areas. Geotechnical Mechanics. 25(S1), 79–82.

[9] Wang, D., 2015. Application of geophysical methods in the detection of goaf in coalfields. Technology Outlook. 25(04), 139.

[10] Mo, L., 2019. Research on comprehensive geophysical exploration method for coal mine goaf in LZC area, Inner Mongolia [PhD thesis]. Xuzhou, China: China University of Mining and Technology. pp. 25–38. DOI: https://doi.org/10.27623/d.cnki.gzkyu.2019.000290

[11] Wang, S., Yang, C., 2015. Bell ringing Selection of detection methods for goaf. Coal Technology. 34(09), 225–228. DOI: https://doi.org/10.13301/j.cnki.ct.2015.09.085

[12] Hu, F., Wu, M., Xu, D., et al., 2018. Using electromagnetic wave CT technology for perspective imaging in karst areas. CT Theory and Application Research. 27(02), 205–212. DOI: https://doi.org/10.15953/j.1004-4140.2018.27.02.09

[13] Liang, C., Huang, H., 2010. Application of inter hole electromagnetic wave perspective and CT scanning in geological exploration of Karst areas. Water Resources Planning and Design. 04, 25–27.

[14] Gan, F., Li, H., Lu, C., et al., 2010. Application of cross hole electromagnetic wave perspective method in detecting and evaluating karst disease foundation of oil storage tanks. Journal of Engineering Geophysics. 7(01), 84–88.

[15] Wu, Y., Chen, Y., Nie, S., 2009. Application of cross hole electromagnetic wave perspective method in Karst exploration of Heyetang elevated bridge. Geophysical and Chemical Exploration. 33(01), 102–104.

[16] Zhang, F., 2008. Application of borehole electromagnetic wave perspective CT technology in the identification of karst caves at the bottom of Jianshan Tunnel. Technology Intelligence Development and Economics. 12, 217–218.

[17] Gan, F., Li, J., Li, H., et al., 2006. Application of cross hole electromagnetic wave perspective method in Karst exploration. Geophysical and Chemical Exploration. 04, 303–307.

[18] Guo, G., Wei, B., 1999. Application of inter well electromagnetic wave CT technology in cave detection. South China Earthquake. 04, 28–34. DOI: https://doi.org/10.13512/j.hndz.1999.04.005

[19] Wang, W., 1983. Application of borehole electromagnetic wave perspective method in engineering geological exploration. Exploration Science and Technology. 01, 6–10.

[20] Wang, W., 1999. Application example of electromagnetic wave perspective in coal mine goaf exploration. Geophysical and Chemical Exploration. 04, 75–77.

[21] Liu, L., Zhao, Z., Li, B., 2021. Tomography of electromagnetic wave attenuation coefficient between coal mine floor holes. Geophysical and Geochemical Exploration Calculation Technology. 43(01), 77–82.

[22] Yorkey, T.J., Webster, J.G., Tompkins, W.L., 1987. Comparing reconstruction algorithms for electrical impendence tomography. IEEE Transaction on Biomedical Engineering. 34(11), 834–852.

[23] Daily, W., Owen, E., 1991. Cross-hole resistivity tomography. Geophysics. 56(8), 1228–1235.

[24] Cheng, J., Lu, Z., Jiang, B., et al., 2022. The "long excavation and long exploration" technology for rapid excavation of coal mine tunnels. Coal Journal. 47(01), 404–412.

[25] Jiang, B., Zhang, P., Cong, L., et al., 2019. Design and implementation of gamma logging control system for borehole direction based on UCOS-II. Coal Technology. 38(08), 158–161 DOI: https://doi.org/10.13301/j.cnki.ct.2019.08.052

[26] Jiang, B., Tian, X., Zhang, P., et al., 2020. Research on the influence of gamma ray on azimuth measurement during borehole and its correction methods. Coal Science and Technology. 48(12), 175–181. DOI: https://doi.org/10.13199/j.cnki.cst.2020.12.022.

[27] Zhang, R., 2016. Research on logging evaluation methods for coalbed methane reservoirs [Ph.D. Thesis]. Changchun, China: Jilin University. pp. 38–48.